Biosensors and Bioelectronics 168 (2020) 112556

Contents lists available at ScienceDirect

Biosensors and Bioelectronics

journal homepage: http://www.elsevier.com/locate/bios

CRISPR/Cas12a-based dual amplified biosensing system for sensitive and rapid detection of polynucleotide kinase/phosphatase

Dong-Xia Wang, Jing Wang, Yi-Chen Du, Jia-Yi Ma, Si-Yuan Wang, An-Na Tang, De-Ming Kong*

State Key Laboratory of Medicinal Chemical Biology, Tianjin Key Laboratory of Biosensing and Molecular Recognition, Research Centre for Analytical Sciences, College of Chemistry, Nankai University, Tianjin, 300071, PR China

ARTICLE INFO

Keywords:
CRISPR/Cas12a
Polynucleotide kinase/phosphatase (PNKP)
Strand displacement amplification
Nicking enzyme
Biosensing

ABSTRACT

We reported a CRISPR/Cas-based dual amplified sensing strategy for rapid, sensitive and selective detection of polynucleotide kinase/phosphatase (PNKP), a DNA damage repair-related biological enzyme. In this strategy, a PNKP-triggered nicking enzyme-mediated strand displacement amplification reaction was introduced to enrich the activator DNA strands for CRISPR/Cas. Such an isothermal DNA amplification step, together with subsequent activated CRISPR/Cas-catalyzed cleavage of fluorescent-labeled short-stranded DNA probes, enable synergetic signal amplification for sensitive PNKP detection. The proposed strategy showed a wide linear detection range (more than 3 orders of magnitude ranging from 1×10^{-5} to 2.5×10^{-2} U/mL T4 PNKP) and a detection limit as low as 3.3×10^{-6} U/mL. It was successfully used for the PNKP activity detection in cell extracts with high fidelity and displayed great potential for enzyme inhibitor screening and inhibitory capability evaluation. This work broadens the applications of CRISPR/Cas12a-based sensors to biological enzymes and provides a way to improve the sensitivity by introducing an isothermal signal amplification step. Such an isothermal DNA amplification-CRISPR/Cas-combined biosensor design concept might expand CRISPR/Cas-based sensing systems and promote their applications in various fields such as disease diagnosis and drug screening.

1. Introduction

Medical early diagnosis is crucial for identifying, preventing and treating multiple diseases, therefore developing accurate, fast and cost-effective sensing strategies for quantifying disease biomarkers are essential (Liu et al., 2020; Topalian et al., 2020; Uckelmann et al., 2020). Although much progress has been made in clinical laboratory testing, new diagnostic techniques with higher sensitivity and better specificity are still urgently needed to improve diagnostic efficiency, develop personalized medicine and thus benefit the entire human health.

Phosphorylation/dephosphorylation of biological macromolecules is widespread in biological systems and plays a vital role in many important physiological processes, such as repairing DNA damage. DNA damage is usually caused by long-term exposure to damaging factors, including ionizing radiation, chemicals and nucleases, it may impact genomic stability, cause chromosomal abnormalities and thus lead to serious consequences. Fortunately, the majority of DNA damages can be repaired spontaneously through multiple DNA repair pathways, in which the participation of multiple enzymes is required (Cui et al., 2019; Li et al., 2018; Zolner et al., 2011). As an indispensable DNA repair enzyme, polynucleotide kinase/phosphatase (PNKP) plays a vital role in DNA recombination, replication and repair, it can catalyze not only the 3′-dephosphorylation but also the 5′-phosphorylation of DNA substrates (Tahbaz et al., 2012; Zhang et al., 2019). Abnormal expression of PNKP activity can inhibit the process of DNA damage repair and cause various human diseases. Therefore, sensitive and rapid quantitative detection of PNKP activity is urgently needed for many aspects such as early diagnosis of diseases and cancer therapy.

The traditional PNKP detection method mainly involves polyacrylamide gel electrophoresis (PAGE) (Meijer et al., 2002), radioisotope ^{32}P labeling (Karimi-Busheri et al., 1998) and autoradiography (Rasouli-Nia et al., 2004). However, these methods may involve the danger of radioactivity, and the operation is time-consuming and laborious. To address these shortcomings, a series of convenient and sensitive sensing strategies have been developed, such as dark-field microscopy (Jin et al., 2020), electrochemistry (Gu et al., 2018; Song

* Corresponding author.
E-mail address: kongdem@nankai.edu.cn (D.-M. Kong).

https://doi.org/10.1016/j.bios.2020.112556
Received 12 July 2020; Received in revised form 14 August 2020; Accepted 24 August 2020
Available online 27 August 2020

et al., 2020; Zhang et al., 2020), chemiluminescence (He et al., 2014), colorimetry and fluorescence (Li et al., 2020; Luo et al., 2020; Wang et al., 2019a; Zhou et al., 2019). Fluorescence-based methods are widely used because of their unique advantages of increased sensitivity, high throughput, facile operation and easy to automation. However, most of the reported fluorescence methods still suffer from the issues of complicated design and unsatisfactory sensitivity due to a lack of efficient signal amplification. Therefore, it is still an urgent need to continuously develop a more sensitive and simpler sensing platform for PNKP activity detection.

Recently, discoveries and researches on gene editing systems based on CRISPR (Clustered Regularly Interspaced Short Palindromic Repeats) have shown great promise for highly sensitive and rapid nucleic acid detection (Li et al., 2019a). The CRISPR-associated (Cas) systems, firstly found in bacteria and archaea, are RNA-guided adaptive immune systems for cleavage of foreign genetic components from invasive viruses and phages (Wan et al., 2019). As a member of the CRISPR family, Cas12a is found to be responsible for both the cleavage of target DNA (termed *cis*-acting cleavage) and the non-specific degradation of non-target single-stranded DNA (termed *trans*-acting cleavage) (Chen et al., 2018; English et al., 2019). Unlike the Cas9 protein, another member of CRISPR family that has been used in biosensing applications (Chen et al., 2020b; Wu et al., 2020), Cas12a endonuclease only needs CRISPR RNA (crRNA) as a guide, eliminating the requirement for trans-activated crRNA (tracrRNA) (Swarts and Jinek, 2018). Therefore, Cas12a is superior to Cas9 in various applications due to its simpler design and more convenient operation (Liang et al., 2019; Wang et al., 2019b, 2020; Zhou et al., 2018), To date, CRISPR/Cas12a-based tools have been widely used in many fields (Dai et al., 2019; Hu et al., 2020; Sun et al., 2020; Xiong et al., 2020; Yuan et al., 2020; Zhao et al., 2020; Zhou et al., 2020), including genome manipulations and biosensing (Chen et al., 2018, 2020a; He et al., 2020). However, most of the reported CRISPR/Cas12a-based biosensors share two limitations: nucleic acid-dominated detection targets and unsatisfactory sensitivity.

Herein, we report a CRISPR/Cas12a-based dual amplified biosensing system for sensitive quantitative detection of PNKP activity, thus successfully extend the application range of CRISPR/Cas12a-based biosensors to biological enzymes. In this strategy, two successive signal amplification steps (nicking enzyme-mediated strand displacement amplification (SDA) and CRISPR/Cas12a-catalyzed DNA probe cleavage) enable PNKP activity detection with high sensitivity. Both two amplification steps are conducted in an isothermal manner and the whole detection can be finished in 80 min, thus conferring the method with the advantages of rapidness and facile operation. Such a sensitive and easy-to-use system was successfully used for the quantitation of PNKP activity in cell lysates, as well as the screening and inhibitory capability evaluation of enzyme inhibitors.

2. Experimental section

2.1. CRISPR/Cas12a-based sensing system for T4 PNKP activity detection

Briefly, a 20 μL reaction mixture containing different concentrations of T4 PNKP, 25 nM of Substrate (Table 1), 2 U/mL of Klenow polymerase, 20 U/mL of Nb.BbvCI, 1 mM of dNTPs, 0.5 × PNKP buffer and 0.5 × cutsmart buffer were incubated at 37 °C for 50 min, followed by heating at 85 °C for 15 min to deactivate T4 PNKP, Klenow and Nb.BbvCI. Then, Cas12a (50 nM), crRNA (60 nM, Table 1), Probe (80 nM, Table 1) were added into the above mixture. After incubation at 37 °C for 10 min, the mixture was supplemented with 80 μL of ultrapure water to give a 100 μL final volume, and its fluorescence spectrum was recorded on a Shimadzu RF-5301 PC fluorescence spectrometer (Shimadzu Ltd., Japan) with an excitation wavelength of 488 nm. Excitation and emission slits were both set at 5.0 nm. In the real-time detection mode, 20 μL of the reaction mixture was prepared and incubated in a commercial StepOnePlus™ Real-Time PCR instrument at 37 °C for 20 min. The fluorescence intensity was collected at 1 min intervals.

In Substrate, the sequences of Part I, II and III are labeled in blue, orange and red, respectively.

2.2. T4 PNKP activity inhibition study

$(NH_4)_2SO_4$ was used as an inhibitor of T4 PNKP to investigate the feasibility of the proposed method for enzyme inhibitor study. The experimental procedures were the same as those of T4 PNKP activity analysis except that T4 PNKP (0.1 U/mL) was pre-incubated with different concentrations of $(NH_4)_2SO_4$ for 10 min before use. The relative activity (*RA*) was calculated according to the following equation:

$$RA = (F_I\text{-}F_b)/(F_0\text{-}F_b) \quad (1)$$

Where F_0 and F_I are the fluorescence signals in the absence and presence of $(NH_4)_2SO_4$, respectively. F_b is the fluorescence intensity of the blank control without T4 PNKP.

2.3. Detection of PNKP activity in HeLa cell lysates

HeLa cells (human cervical cancer cell line) were used as the model cell line for PNKP activity analysis in cells. HeLa cells were cultured in Dulbecco's modified Eagle's medium (DMEM, Gibco) (containing 10% bovine serum albumin and 1% penicillin-streptomycin) at 37 °C under 5% CO_2. The cell lysates were prepared using a nucleoprotein extraction kit (Sangon Biotech, Shanghai, China). Briefly, approximately 1×10^7 HeLa cells were washed with 1 × PBS buffer twice and centrifuged at 1000 rpm for 4 min. Then, 500 μL lysis buffer was added and the mixture sample was lysed on ice for 30 min, shaking for 15 s every 5 min. The obtained mixture sample was centrifuged (12,000 rpm) for 20 min at 4 °C, and the supernatant was divided and stored at −20 °C until use. The quantitative detection of enzyme activity was performed as above, except that HeLa cell lysates were added to the sensing platform instead

Table 1
Sequences of the oligonucleotides used in this work.

Oligonucleotide	Sequences (5' to 3')
Substrate	AGTTTCTGAAGTAGATATGGCAGCACATAATG*CCTCAGC*CGCA CCACTAAAGTGGTGCG-PO_4
Activator DNA	TGAGGCATTATGTGCTGCCATATCTACTTCAGAAACT
crRNA	UAAUUUCUACUAAGUGUAGAUGAAGUAGAUAUGGCAGCAC
Probe	FAM-TTATT-BHQ1
FAM-ssDNA	FAM- TCATGTTTGTTTGTTGGCCCCCCTTCTTTCTTA

of T4 PNKP.

3. Results and discussion

3.1. Design of CRISPR/Cas12a-based PNKP-sensing strategy

In our proposed dual amplified sensing strategy (Scheme 1 and Fig. 1A), a substrate DNA (Substrate in Table 1) with an incomplete double-stranded DNA (dsDNA) structure is used. This substrate DNA contains three parts. Part I, located at the 3′-side of the substrate, folds into a hairpin structure and its 3′-end is modified with a phosphate group; Part III, located at the 5′-side of the substrate, is a single-stranded sequence, whose complementary sequence can recognize the Cas12a/crRNA complex and activate the *trans*-cleavage activity of Cas12a/crRNA; Part I and III are separated by the recognition site of nicking endonuclease (Nb.BbvCI) (Part II). With the addition of PNKP, the 3′-phosphate group of the substrate DNA can be hydrolyzed to a hydroxyl group, and then extended by Klenow fragment DNA polymerase (abbreviated as Klenow) to form an extension product with intact dsDNA structure. Next, the extension product is nicked at the recognition site by the nicking endonuclease Nb.BbvCI, and the newly generated 3′-end is extended again by Klenow, thus starting the nicking-polymerization-displacement cycle of the SDA reaction. The accumulated single-stranded reaction products (denoted as "activator DNA") can then initiate the *trans*-cleavage activity of Cas12a/crRNA to trigger the second round of signal amplification, in which the fluorophore/quencher pair-labeled short-stranded DNA probes (Probe in Table 1) are cleaved. As a result, the previously quenched fluorescence is turned on. According to the change of fluorescence value in the sensing system, the PNKP activity can be accurately quantified. In the absence of PNKP, however, the 3′-end of the substrate DNA cannot be extended by Klenow due to the presence of 3′-phosphate group. Therefore, the two rounds of signal amplification will not be initiated, and the fluorescence of the sensing system barely changes (Jiang et al., 2014).

3.2. Feasibility analysis of the CRISPR/Cas12a-based sensing strategy

To verify the feasibility of the CRISPR/Cas12a-based sensing strategy, PAGE analysis was used to demonstrate the successful implementation of the two rounds of signal amplification reactions. As shown in Fig. 1C, without T4 PNKP, the 3′-end of the substrate DNA cannot be extended by Klenow or Nb.BbvCI due to the presence of 3′-phosphate group (Lanes 1–3). In the presence of T4 PNKP, however, the substrate was extended by Klenow to form an extension product with an intact dsDNA structure, resulting in a much brighter DNA band with lower mobility than the incomplete dsDNA (Lane 4). With the further addition of Nb.BbvCI, a new band corresponding to single-stranded activator DNA emerged (Lane 5), thus demonstrating the successful implementation of the SDA cycle. Because the staining capability of ethidium bromide (EB) to single-stranded DNA (ssDNA) is much lower than that to dsDNA, a relatively pale band was given by the activator DNA.

To demonstrate that the SDA products can activate the ssDNA

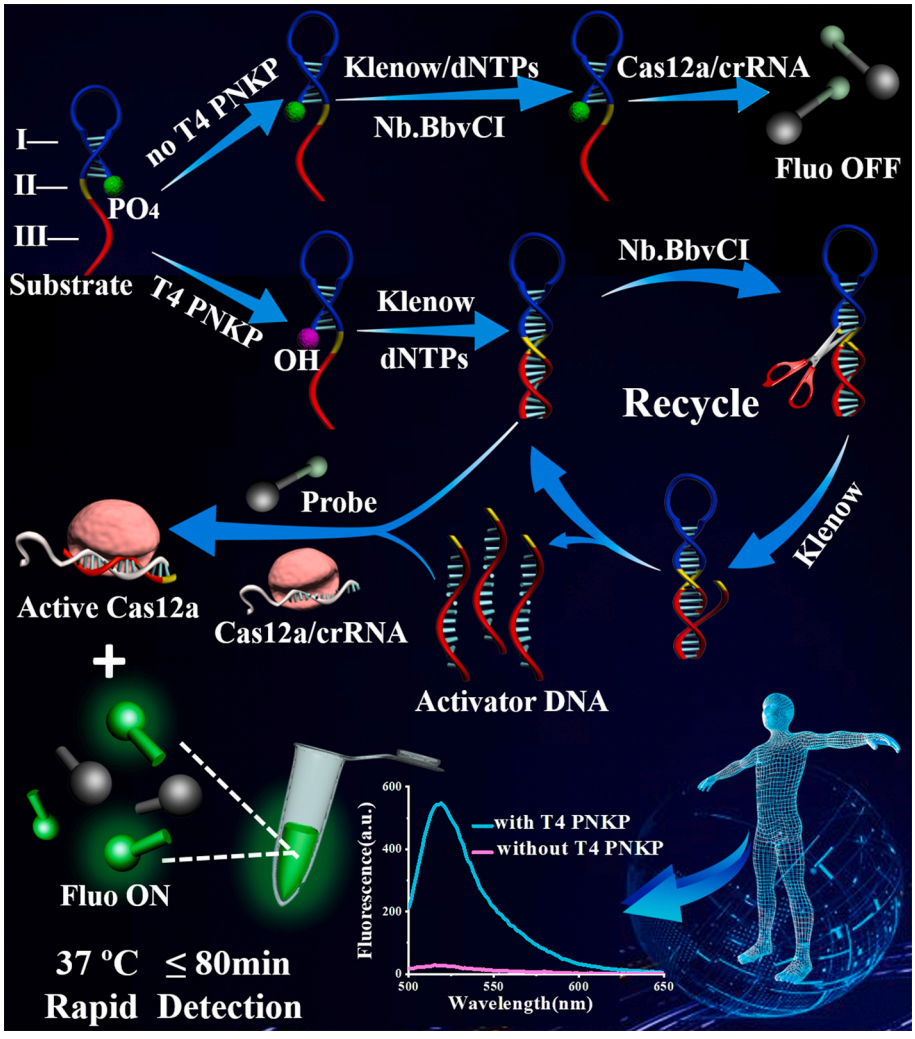

Scheme 1. Schematic of CRISPR/Cas12a-based biosensing platform for sensitive and rapid detection of PNKP activity.

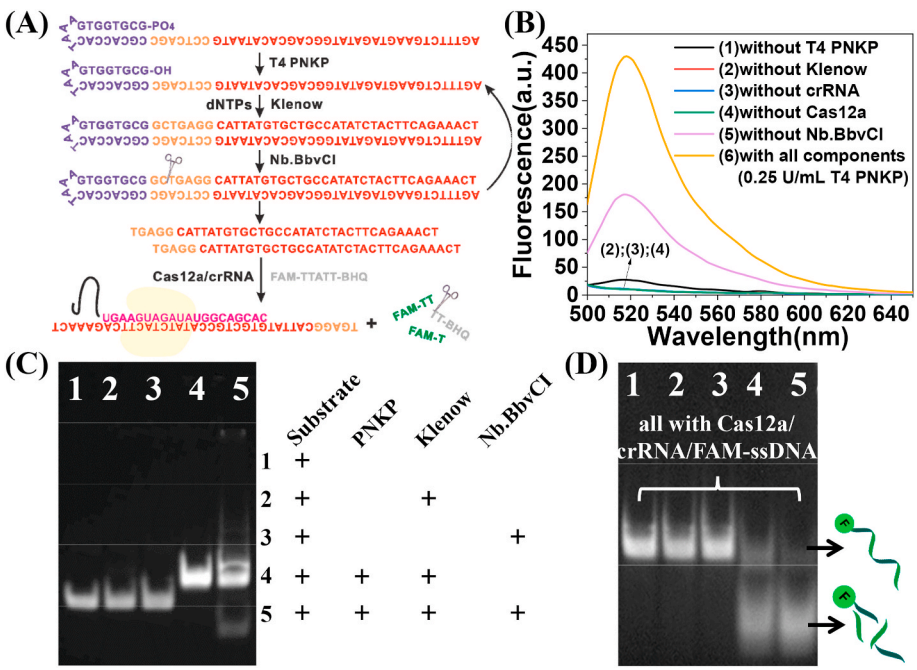

Fig. 1. Feasibility analysis of the proposed CRISPR/Cas12a-based PNKP-sensing strategy. (A) The detailed working mechanism in which DNA and RNA sequences are given. (B) Fluorescence spectra of different sensing systems. (C) Non-denaturing PAGE characterization of nicking enzyme-mediated SDA. Lane 1: Substrate; Lane 2: Substrate + Klenow; Lane 3: Substrate + Nb.BbvCI; Lane 4: Substrate + T4 PNKP + Klenow; Lane 5: Substrate + T4 PNKP + Klenow + Nb.BbvCI. The gel was photographed after staining by EB for 15 min. (D) Non-denaturing PAGE characterization of SDA products-triggered activation of Cas12a/crRNA. Lanes 1–5 were the same as (C) except that FAM-ssDNA and Cas12a/crRNA were added. The gel was photographed directly by utilizing the fluorescence of FAM-ssDNA.

cleavage activity of Cas12a/crRNA, a fluorophore-labeled ssDNA probe (FAM-ssDNA, Table 1) with 33 nucleotides was designed and added in above five systems together with Cas12a/crRNA. As shown in Fig. 1D, without the addition of T4 PNKP, FAM-ssDNA keeps intact (Lanes 1–3). After the addition of T4 PNKP, however, the amount of intact FAM-ssDNA decreased, accompanied by the emergence of a broad DNA band with faster mobility (Lane 4), suggesting that FAM-ssDNA has been cleaved into short pieces. This result indicated that dsDNA containing activator DNA sequence can also activate the DNA cleavage activity of Cas12a/crRNA, which is consistent with previous reports (Chen et al., 2018; Li et al., 2019b). Further addition of Nb.BbvCI resulted in the cleavage of more FAM-ssDNA strands (Lane 5), which is caused by the combined activation of Cas12a/crRNA by double-stranded and single-stranded products. The activation ability of a single-stranded product was further demonstrated by the artificially synthetic activator DNA strand (Fig. S1).

Next, a 5-nt dual-labeled ssDNA probe, in which the fluorophore and quencher are quite close to each other, was added instead of FAM-ssDNA, and the fluorescence spectra of different sensing systems were recorded. As shown in Fig. 1B, only the two systems containing T4 PNKP, Klenow and Cas12a/crRNA complex showed increased fluorescence compared to the negative controls without T4 PNKP, Klenow, Cas12a or crRNA. Besides, in the two positive systems, the one with Nb.BbvCI gave much higher fluorescence than that without Nb.BbvCI, highlighting the signal amplification capability of nicking enzyme-mediated SDA. In the four tested negative controls, the one without T4 PNKP exhibited a low background fluorescence, which might be attributed to the presence of a tiny amount of unphosphorylated substrate DNA. This result, from another angle, also reflects the excellent signal amplification ability of the proposed fluorescent sensing platform.

3.3. Sensitivity and selectivity of T4 PNKP activity analysis

To achieve the best CRISPR/Cas12a based-T4 PNKP-sensing performance, some critical experimental conditions were optimized (Figs. S2–S10). Through repeated optimization, the optimal reaction condition was obtained: 25 nM of Substrate; 2 U/mL of Klenow; 20 U/mL of Nb.BbvCI; 50 nM of Cas12a; 60 nM of crRNA; 80 nM of Probe and 1 mM of dNTPs, 10 min for Probe cleavage, 0.5 × PNKP buffer +0.5 × cutsmart buffer. Then, the performance of this detection method in T4 PNKP activity analysis was detected. Fig. 2A shows the fluorescence signal change as a function of T4 PNKP concentration in the range of 0–1 U/mL. As expected, the sensor system gave a T4 PNKP concentration-dependent fluorescence change, and a linear relationship (R^2 = 0.9916) was observed between the fluorescence signal and the logarithm of T4 PNKP concentration ranging from $1 \times 10^{-5} - 2.5 \times 10^{-2}$ U/mL (Fig. 2B). The detection limit was calculated to be 3.3×10^{-6} U/mL based on a 3σ/slope (σ is the standard deviation of ten blank samples), which is equal to or lower than other reported results (Table S1), thus demonstrating the high sensitivity of our method. By fixing the T4 PNKP concentration at 0.1 U/mL, the reproducibility of our method was evaluated. The relative standard deviations (RSD) of the intra- (3.49%) and intergroup (4.36%) were both lower than 5%, indicating that our biosensing system has good reproducibility. Besides the end-point detection, the fluorescence signal changes can also be easily monitored in real-time due to the isothermal characteristic of the signal amplification reactions. Both time and T4 PNKP concentration-dependent fluorescence changes were given in such a real-time mode (Fig. S11). According to the linear relationship between the RT_t value (reaction time when the fluorescence intensity reaches the set threshold) and the logarithm of T4 PNKP concentration, the T4 PNKP activity could also be sensitively detected. The real-time detection mode can further simplify the detection operations, thereby enabling high throughput detection possible (Du et al., 2016).

To increase the sensitivity of the CRISPR/Cas12a-based sensing system, we added a nicking enzyme-mediated SDA reaction to magnify subsequent Cas12a/crRNA-catalyzed probe cleavage reaction. To highlight the contribution of the nicking enzyme-mediated SDA reaction to detection sensitivity, the T4 PNKP-sensing performances of the two sensing systems with or without Nb.BbvCI were compared. In the absence of Nb.BbvCI, T4 PNKP-dependent dephosphorylated substrate DNA will be extended by DNA polymerase to form intact double-

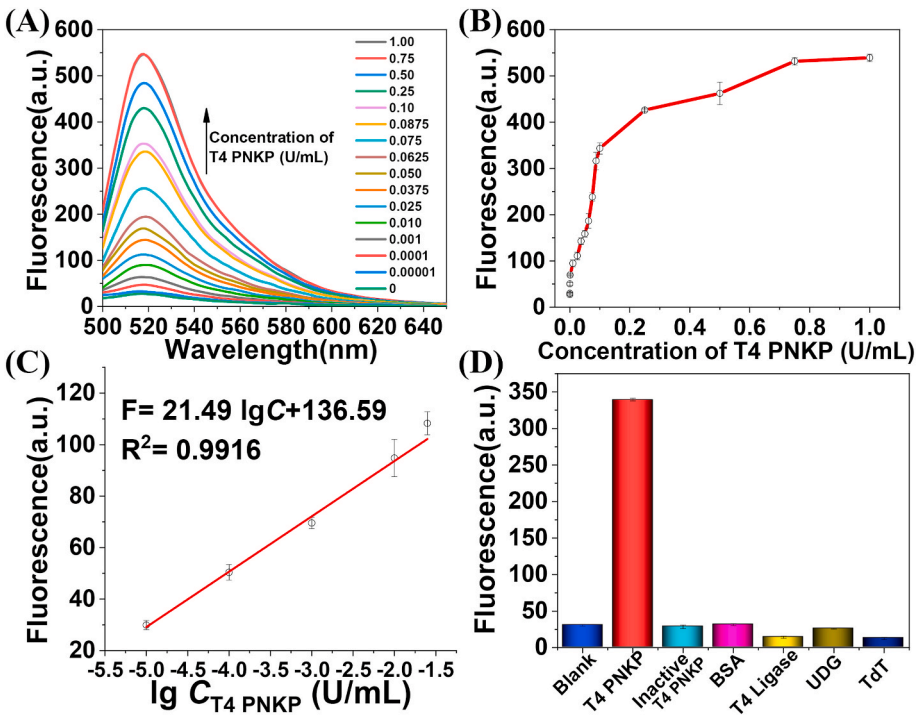

Fig. 2. Quantitation of T4 PNKP activity in end-point mode. (A) Fluorescence spectrum of the system containing varying amounts of T4 PNKP. (B) T4 PNKP concentration-dependent changes in the fluorescence intensity at 520 nm. (C) The linear relationship between fluorescence and the logarithm of T4 PNKP concentration in the range of $1 \times 10^{-5} - 2.5 \times 10^{-2}$ U/mL. Error bars represent the standard deviation of three repetitive experiments. (D) Selectivity of the T4 PNKP activity analysis method. [T4 PNKP] = 0.1 U/mL, [BSA] = 20 mg/mL, [T4 ligase] = [UDG] = [TdT] = 10 U/mL. Inactive T4 PNKP was prepared by heating the enzyme at 85 °C for 15 min.

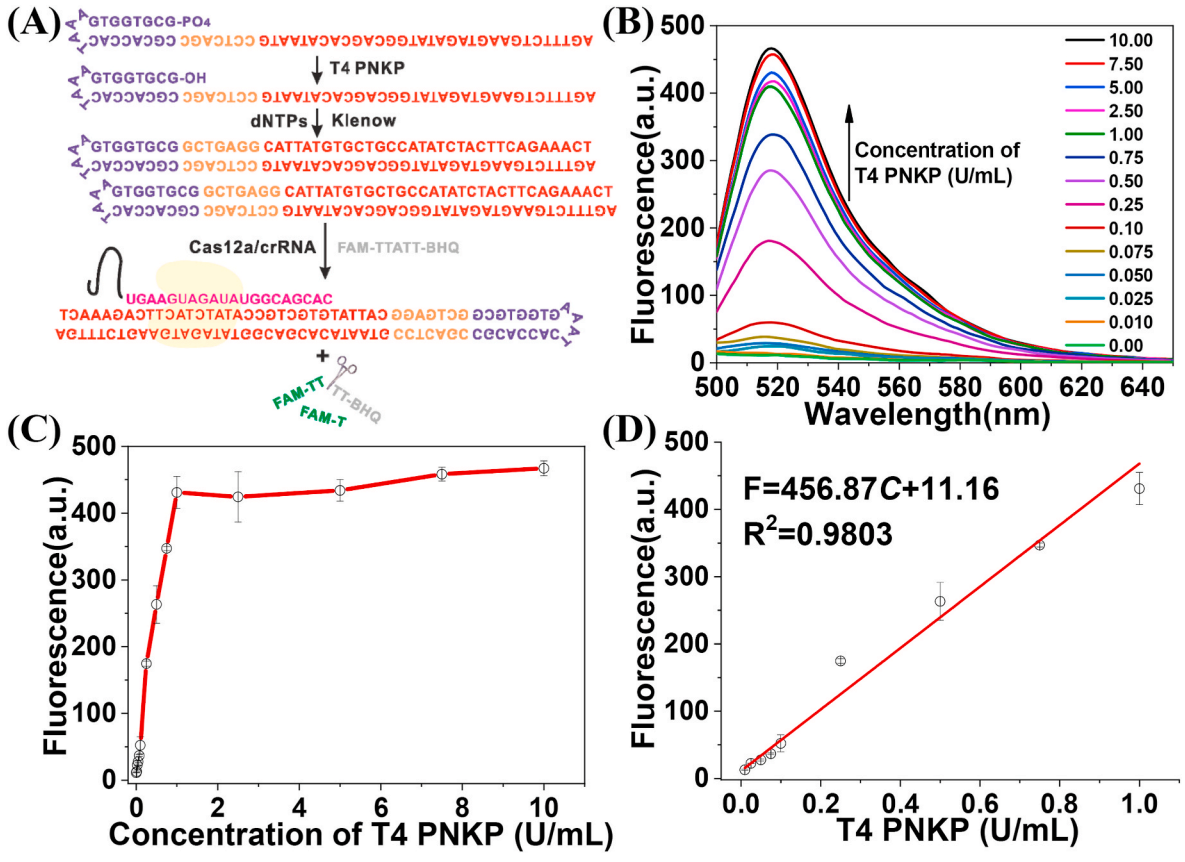

Fig. 3. Quantitation of T4 PNKP using the CRISPR/Cas12a-based sensing platform without Nb.BbvCI addition. (A) Detailed working mechanism in which DNA and RNA sequences are given. (B) Fluorescence spectrum of the sensing system containing varying amounts of T4 PNKP. (C) T4 PNKP concentration-dependent changes in the fluorescence intensity at 520 nm. (D) The linear relationship between the fluorescence intensity and T4 PNKP concentration in the range of $1 \times 10^{-2} - 1$ U/mL. Error bars represent the standard deviation of three repetitive experiments.

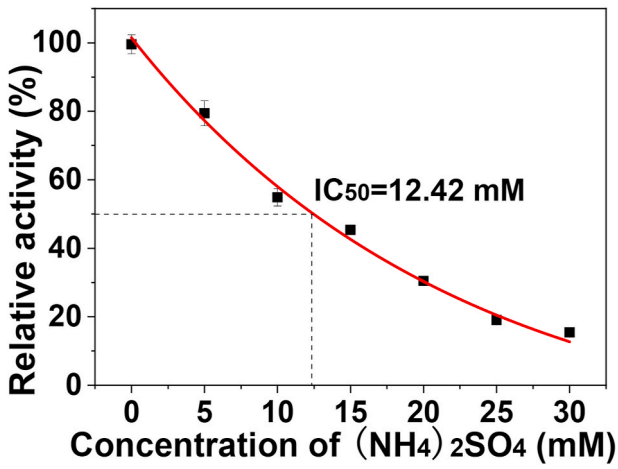

Fig. 4. Inhibition of PNKP activity by $(NH_4)_2SO_4$. [T4 PNKP] = 0.1 U/mL. PNKP activity analysis in cell lysates.

stranded product, but no single-stranded activator DNA is produced. Since the intact double-stranded product can also activate the DNA cleavage activity of Cas12a/crRNA (Fig. 3A), quantitation of T4 PNKP can be achieved with a linear detection range of 0.01–1 U/mL (Fig. 3B–D). The detection limit was calculated to be 3.3×10^{-3} U/mL, which is 3 orders higher than that of the sensing system with Nb.BbvCI addition.

The proposed sensing strategy shows excellent selectivity towards T4 PNKP. To demonstrate this, the fluorescence response of the sensing platform to competitive enzymes and proteins, including terminal deoxynucleotidyl transferase (TdT), bovine serum albumin (BSA), T4 ligase and uracil DNA glycosylase (UDG) were tested. None of them showed a detectable increase in fluorescence signal compared with the blank control (Fig. 2D). After heating at 85 °C for 15 min, the obtained heat-inactivated T4 PNKP lost the ability to increase the fluorescence of the sensing platform, confirming that the fluorescence response of the sensing system is associated with the enzyme activity of T4 PNKP. Collectively, the above experimental results prove that our sensing platform is very feasible for the rapid, highly sensitive and selective detection of T4 PNKP activity.

3.4. Inhibition assay of T4 PNKP activity

PNKP is a versatile enzyme that can be used for many DNA damage repair pathways, its abnormal expression is closely related to various human diseases. Inhibition of PNKP activity has been reported as a potential pathway of cancer therapy, while also increasing the sensitivity of cancer cells to radiation therapy and chemotherapy (Du et al., 2019; Jiang et al., 2014, 2018). Therefore, screening of PNKP inhibitors and evaluating their inhibitory capabilities have important implications for cancer treatment. In addition to ultra-sensitive detection of PNKP activity, our CRISPR/Cas-based sensing system can also be used to facilely evaluate the inhibitory abilities of PNKP inhibitors. To demonstrate this, ammonium sulfate $(NH_4)_2SO_4$ was selected as the model inhibitor. When adding different concentrations of $(NH_4)_2SO_4$ to the sensing systems containing 0.1 U/mL T4 PNKP, $(NH_4)_2SO_4$ dose-dependent fluorescence decrease was observed (Fig. 4). Since the activities of Klenow, Nb.BbvCI and Cas12a/crRNA were barely affected by $(NH_4)_2SO_4$ (Fig. S12), the observed fluorescence decrease was indeed related with the inhibition of T4 PNKP activity by $(NH_4)_2SO_4$. IC_{50} value, the inhibitor concentration that inhibits the T4 PNKP activity by about 50%, was calculated to be 12.42 mM, which close to those reported in the literatures (Xiong et al., 2020; Sun et al., 2020), suggesting our proposed CRISPR/Cas12a sensing system can also be used to screen T4 PNKP inhibitors and evaluate their inhibitory capacity, thereby providing the possibility in drug discovery of PNKP-related diseases.

To demonstrate the potential application of our CRISPR/Cas12a-based sensing system in complex and real biological samples, the PNKP activity in cancer cell lysates was analyzed. When the lysates of 1000 HeLa cells were added in the sensing system, the fluorescence

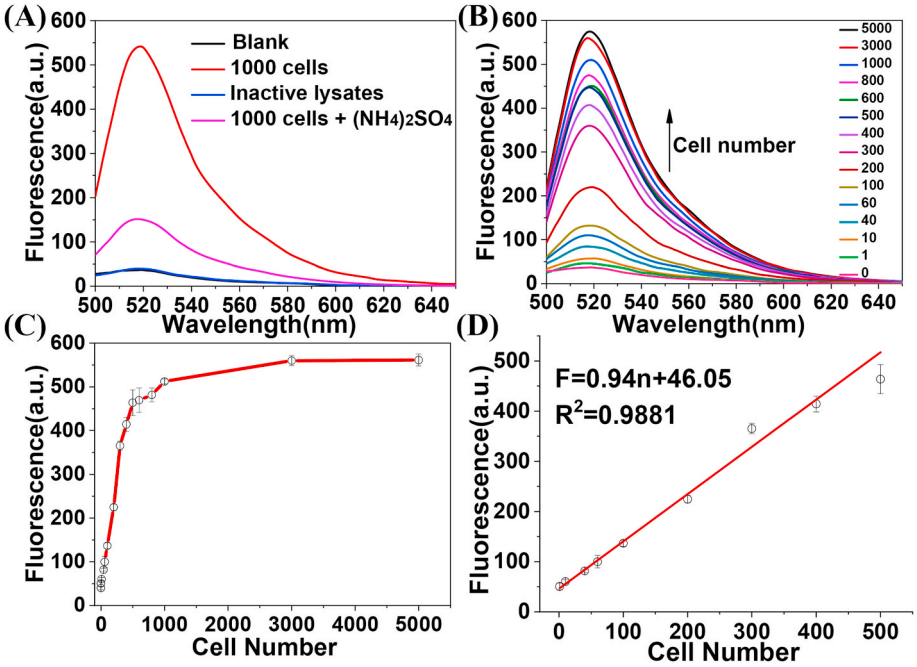

Fig. 5. PNKP activity analysis in HeLa cell lysates. (A) Fluorescence spectra of several sensing platforms. Cell lysates were extracted from 1000 HeLa cells. $[(NH_4)_2SO_4]$ = 20 mM. (B) Fluorescence spectrum of the sensing system containing different numbers of HeLa cells. (C) The changes in fluorescence intensity at 520 nm as a function of the HeLa cell number. (D) The linear relationship between the fluorescence intensity and the HeLa cell number in the range of 1–500 cells.

increased significantly. Because other complex components in the cell lysates may interfere with the judgment of the results, to confirm the observed high fluorescence signal was indeed caused by the active PNKP in the cell lysates, PNKP inhibitor $(NH_4)_2SO_4$ was added in the HeLa cell lysates. As shown in Fig. 5A, the fluorescence signal was greatly reduced due to the inhibition of T4 PNKP activity. When the PNKP activity of the cell lysates was inactivated by heating at 95 °C for 30 min, the heat-inactivated cell lysates also could not cause a detectable fluorescence signal at all. These results demonstrate that the significant increase in fluorescence signal caused by cell lysates is closely related to active PNKP.

Then, the sensitivity of the sensing platform for quantifying PNKP activity in HeLa cell lysates was investigated. As shown in Fig. 5B, the fluorescence intensity continuously increased with cell number, and even one cell could give a fluorescence response distinguishable from that of the blank control. A linear relationship was observed between the fluorescence intensity and cell number in the range of 1–500 cells (Fig. 5C and D). Based on the fluorescence displayed by 500 cells, the PNKP activity in HeLa cells was estimated to be 3.4×10^{-4} U/cell, which is comparable to the result reported in the literature (Hu et al., 2019). It is worth noting that this method can rapidly analyze endogenous PNKP activity at the single-cell level, thus showing great potential in biomedicine and early diagnosis.

4. Conclusion

In summary, we reported a CRISPR/Cas12a-based fluorescent sensing system for the rapid, sensitive and selective detection of PNKP activity. Due to the synergy of two successive signal amplification steps, the proposed method shows ultrahigh detection sensitivity with a detection limit as low as 3.3×10^{-6} U/mL, and the linear detection range spans more than 3 orders of magnitude ranging from 1×10^{-5} U/mL to 2.5×10^{-2} U/mL. Constant reaction temperature greatly simplifies the detection operation and eliminates the requirement for complicated instruments, and the whole detection operation can be finished in 80 min. The proposed sensing system was successfully used for the PNKP activity detection in cell extracts with high fidelity and showed great potential for the enzyme inhibitor screening and inhibitory capability evaluation. This work broadens the applications of CRISPR/Cas12a-based sensors from nucleic acid targets to biological enzymes. By designing different SDA-initiating mechanisms, this dual-amplified CRISPR/Cas12a-based sensing platform can be easily extended to the quantitation of other targets such as UDG, DNA methyltransferase and so on (Du et al., 2016, 2019; Huang et al., 2017). This work demonstrates that the sensitivity of CRISPR/Cas12a-based sensors can be greatly improved by introducing a simple isothermal DNA amplification step to enrich activator DNA strands for Cas12a/crRNA. Such a designing concept might also be feasible for other isothermal DNA amplification techniques, thus will expand the design of CRISPR/Cas12a-based sensors and promote their applications in various fields.

CRediT authorship contribution statement

Dong-Xia Wang: Conceptualization, Methodology, Investigation, Writing - original draft. **Jing Wang:** Visualization, Investigation. **Yi-Chen Du:** Investigation. **Jia-Yi Ma:** Investigation. **Si-Yuan Wang:** Validation. **An-Na Tang:** Supervision, Writing - review & editing. **De-Ming Kong:** Supervision, Writing - review & editing.

Declaration of competing interest

The authors declare that they have no known competing financial interests or personal relationships that could have appeared to influence the work reported in this paper.

Acknowledgment

This work was supported by the National Natural Science Foundation of China (No. 21874075) and the Fundamental Research Funds for Central University, Nankai University (No. 63201043).

Appendix A. Supplementary data

Supplementary data to this article can be found online at https://doi.org/10.1016/j.bios.2020.112556.

References

Chen, J.S., Ma, E., Harrington, L.B., Da Costa, M., Tian, X., Palefsky, J.M., Doudna, J.A., 2018. Science 360, 436–439.
Chen, X., Cao, G., Wang, X., Ji, Z., Xu, F., Huo, D., Luo, X., Hou, C., 2020a. Biosens. Bioelectron. 163, 112271.
Chen, X., Wu, Y., Cao, G., Wang, X., Ji, Z., Huo, D., Xu, F., Hou, C., 2020b. ACS Sens. 5, 1615–1623.
Cui, Y.X., Feng, X.N., Li, X.Y., Zhang, Y.P., Tang, A.N., Kong, D.M., 2019. Chem. Commun. 55, 7603–7606.
Dai, Y., Somoza, R.A., Wang, L., Welter, J.F., Li, Y., Caplan, A.I., Liu, C.C., 2019. Angew. Chem. Int. Ed. 58, 2–9.
Du, Y.C., Wang, S.Y., Li, X.Y., Wang, Y.X., Tang, A.N., Kong, D.M., 2019. Biosens. Bioelectron. 145, 111700.
Du, Y.C., Zhu, L.N., Kong, D.M., 2016. Biosens. Bioelectron. 86, 811–817.
English, M.A., Soenksen, L.R., Gayet, R.V., de Puig, H., Angenent-Mari, N.M., Mao, A.S., Nguyen, P.Q., Collins, J.J., 2019. Science 365, 780–785.
Gu, C., Gai, P., Han, L., Yu, W., Liu, Q., Li, F., 2018. Chem. Commun. 54, 5438–5441.
He, H.Z., Leung, K.H., Wang, W., Chan, D.S., Leung, C.H., Ma, D.L., 2014. Chem. Commun. 50, 5313–5315.
He, Q., Yu, D., Bao, M., Korensky, G., Chen, J., Shin, M., Kim, J., Park, M., Qin, P., Du, K., 2020. Biosens. Bioelectron. 154, 112068.
Hu, M., Yuan, C., Tian, T., Wang, X., Sun, J., Xiong, E., Zhou, X., 2020. J. Am. Chem. Soc. 142, 7506–7513.
Huang, J., Li, X.Y., Du, Y.C., Zhang, L.N., Liu, K.K., Zhu, L.N., Kong, D.M., 2017. Biosens. Bioelectron. 91, 417–423.
Jiang, H., Xu, Y., Dai, L., Liu, X., Kong, D., 2018. Sens. Actuators, B 260, 70–77.
Jiang, H.X., Kong, D.M., Shen, H.X., 2014. Biosens. Bioelectron. 55, 133–138.
Jin, T., Zhang, J., Zhao, Y., Huang, X., Tan, C., Sun, S., Tan, Y., 2020. Biosens. Bioelectron. 150, 111936.
Karimi-Busheri, F., Lee, J., Weinfeld, M., Tomkinson, A.E., 1998. Nucleic Acids Res. 26, 4395–4400.
Li, X.Y., Cui, Y.X., Du, Y.C., Tang, A.N., Kong, D.M., 2020. Analyst 145, 3742–3748.
Li, X.Y., Du, Y.C., Pan, Y.N., Su, L.L., Shi, S., Wang, S.Y., Tang, A.N., Kim, K., Kong, D.M., 2018. Chem. Commun. 54, 13841–13844.
Li, Y., Li, S., Wang, J., Liu, G., 2019a. Trends Biotechnol. 37, 730–743.
Li, Y., Mansour, H., Wang, T., Poojari, S., Li, F., 2019b. Anal. Chem. 91, 11510–11513.
Liang, M., Li, Z., Wang, W., Liu, J., Liu, L., Zhu, G., Karthik, L., Wang, M., Wang, K.F., Wang, Z., Yu, J., Shuai, Y., Yu, J., Zhang, L., Yang, Z., Li, C., Zhang, Q., Shi, T., Zhou, L., Xie, F., Dai, H., Liu, X., Zhang, J., Liu, G., Zhuo, Y., Zhang, B., Liu, C., Li, S., Xia, X., Tong, Y., Liu, Y., Alterovitz, G., Tan, G.Y., Zhang, L.X., 2019. Nat. Commun. 10, 3672.
Liu, J., Kim, Y.S., Richardson, C.E., Tom, A., Ramakrishnan, C., Birey, F., Katsumata, T., Chen, S., Wang, C., Wang, X., Joubert, L.-M., Jiang, Y., Wang, H., Fenno, L.E., Tok, J. B.H., Paşca, S.P., Shen, K., Bao, Z., Deisseroth, K., 2020. Science 367, 1372.
Luo, R., Zhou, H., Dang, W., Long, Y., Tong, C., Xie, Q., Daniyal, M., Liu, B., Wang, W., 2020. Sens. Actuators, B 310, 127884.
Meijer, M., Karimi-Busheri, F., Huang, T.Y., Weinfeld, M., Young, D., 2002. J. Biol. Chem. 277, 4050–4055.
Rasouli-Nia, A., Karimi-Busheri, F., Weinfeld, M., 2004. Proc. Natl. Acad. Sci. U.S.A. 101, 6905–6910.
Song, Z., Li, Y., Teng, H., Ding, C., Xu, G., Luo, X., 2020. Sens. Actuators, B 305, 127329.
Sun, W., Wang, J., Hu, Q., Zhou, X., Khademhosseini, A., Gu, Z., 2020. Sci. Adv. 6, eaba2983.
Swarts, D.C., Jinek, M., 2018. WIREs RNA 9, e1481.
Tahbaz, N., Subedi, S., Weinfeld, M., 2012. Nucleic Acids Res. 40, 3484–3495.
Topalian, S.L., Taube, J.M., Pardoll, D.M., 2020. Science 367, eaax0182.
Uckelmann, H.J.K., Stephanie, M., Wong, Eric M., Hatton, C., Giovinazzo, H., Gadrey, J. Y., Krivtsov, A.V., Rücker, F.G., Döhner, K., McGeehan, G.M., Levine, R.L., Bullinger, L., Vassiliou, G.S., Armstrong, S.A., 2020. Science 367, 586.
Wan, T., Niu, D., Wu, C., Xu, F., Church, G., Ping, Y., 2019. Mater. Today 26, 40–66.
Wang, M., Kong, D., Su, D., Liu, Y., Su, X., 2019a. Nanoscale 11, 13903–13908.
Wang, T., Liu, Y., Sun, H.H., Yin, B.C., Ye, B.C., 2019b. Angew. Chem. Int. Ed. 58, 5382–5386.
Wang, X., Xiong, E., Tian, T., Cheng, M., Lin, W., Wang, H., Zhang, G., Sun, J., Zhou, X., 2020. ACS Nano 14, 2497–2508.
Wu, H., Qian, C., Wu, C., Wang, Z., Wang, D., Ye, Z., Ping, J., Wu, J., Ji, F., 2020. Biosens. Bioelectron. 157, 112153.
Xiong, Y., Zhang, J., Yang, Z., Mou, Q., Ma, Y., Xiong, Y., Lu, Y., 2020. J. Am. Chem. Soc. 142, 207–213.

Yuan, C., Tian, T., Sun, J., Hu, M., Wang, X., Xiong, E., Cheng, M., Bao, Y., Lin, W., Jiang, J., Yang, C., Chen, Q., Zhang, H., Wang, H., Wang, X., Deng, X., Liao, X., Liu, Y., Wang, Z., Zhang, G., Zhou, X., 2020. Anal. Chem. 92, 4029–4037.
Zhang, G., Chai, H., Tian, M., Zhu, S., Qu, L., Zhang, X., 2020. Anal. Chem. 92, 7354–7362.
Zhang, Y.P., Cui, Y.X., Li, X.Y., Du, Y.C., Tang, A.N., Kong, D.M., 2019. Chem. Commun. 55, 7611–7614.
Zhao, X., Zeng, L., Mei, Q., Luo, Y., 2020. ACS Sens. 5, 2239–2246.
Zhou, H., Tong, C., Zou, W., Yang, Y., Liu, Y., Li, B., Qin, Y., Dang, W., Liu, B., Wang, W., 2019. Analyst 144, 1187–1196.
Zhou, R., Li, Y., Dong, T., Tang, Y., Li, F., 2020. Chem. Commun. 56, 3536–3538.
Zhou, W., Hu, L., Ying, L., Zhao, Z., Chu, P.K., Yu, X.F., 2018. Nat. Commun. 9, 5012.
Zolner, A.E., Abdou, I., Ye, R., Mani, R.S., Fanta, M., Yu, Y., Douglas, P., Tahbaz, N., Fang, S., Dobbs, T., Wang, C., Morrice, N., Hendzel, M.J., Weinfeld, M., Lees-Miller, S.P., 2011. Nucleic Acids Res. 39, 9224–9237.